Indonesian J. Pharm. Vol. 26 No. 3 : 147 – 157
ISSN-p : 2338-9427
DOI: 10.14499/indonesianjpharm26iss3pp147

Research Article

NARINGENIN-LOADED CHITOSAN NANOPARTICLES FORMULATION, AND ITS *IN VITRO* EVALUATION AGAINST T47D BREAST CANCER CELL LINE

Lina Winarti[1] , Lusia Oktora Ruma Kumala Sari[1], Agung Endro Nugroho[2*]

[1]Dept of Pharmaceutics, Faculty of Pharmacy, University of Jember, Jember 68121, Indonesia;
[2]Dept of Pharmacology and Clinical Pharmacy, Faculty of Pharmacy, Universitas Gadjah Mada, Yogyakarta 55281, Indonesia.

Submitted: 02-04-2015
Revised: 11-05-2015
Accepted: 22-06-2015

*Corresponding author
Agung Endro Nugroho

Email:
agungendronugroho@gmail.com

ABSTRACT

Naringenin (NAR), a natural flavonoid aglycone of naringin has been extensively investigated for its pharmacological activities, including anti-tumor effects. However, its poor bioavailability has been identified as the single most important challenge in oral drug delivery. Based in this condition, it is used nanoencapsulation to increase the effectiveness of NAR as anti-cancer. The objectives of this research were to develop the formulation of NAR-loaded nanoparticles (NARNPs) as well as to evaluate its potential as anti-cancer against T47D breast cancer cells line. NARNPs is prepared through the method of ionic gelation, meanwhile its characteristic is evaluated through photon correlation spectroscopy (PCS), transmission electron microscopy (TEM), fourier transform infra-red spectroscopy (FTIR), and different scanning calorimeter (DSC). The result of MTT test and cellular uptake indicate that NARNPs increase cytotoxicity and internalization of NAR to the cells compared to that of free NAR. The result of qualitative apoptosis study using fluorescence microscope indicates that both free NAR and NARNPs were able to induce apoptosis. It can be conclude that Chitosan nanoparticles–TPP conjugates have the capability to encapsulate naringenin hence increase the cellular uptake and cytotoxcicity of naringenin against T47D cell line. NARNPs also could induce the apoptosis effect.

Keywords: NAR, Chitosan (CS), ionic gelation, nanoparticles

INTRODUCTION

NAR (4',5,7-trihydroxyflavanone) is a compound included in flavonoid class. This compound originally comes from orange (*Citrus reticulate* and *Citrus aurantum*) (De Leo and De Bosco, 2005; Tripoli *et al.,* 2007) and is frequently distributed in citrus fruit (Dembinski *et al.,* 2004), tomatoes (Le Gall *et al.,* 2003), cherries (Wang *et al.,* 1999), grapefruit (Erlund *et al.,* 2001), and cocoa (Stark *et al.,* 2005). It has a character of not being dissolved in water because it is an aglycone. NAR is a chemopreventive agent that has been proven of being cytotoxic to the gastric cancer cells (KATOIII and MKN-7) and liver cancer cells (HepG2,Hep3B, Huh7) by inducting apoptosis through different pathway from p53 (Kanno *et al.,* 2005; Chang *et al.,* 2008). In addition, NAR is also able to induce apoptosis through inducing activation of NF-kB on HL-60 cells as well as activation of p38 MAPK and JNK1/2 (Kanno *et al.,* 2005; Kanno *et al.,* 2006; Gopalakrishnan *et al.,* 2006)

NAR has been used as doxorubicin co-chemotheraphy (Junedi *et al.,* 2010). Doxorubicin usage in the long term has a potential to cause cardiotoxicity and insensitivity of cancer cells on doxorubicin. NAR is able to induce apoptosis through different pathway from p53 (Zhang *et al.,* 2009), therefore it is able to increase cancer cell sensitivity that has been resistant to doxorubicin as well as to cancer cell which has mutated p53 characteristic (Junedi *et al.,* 2010; Fitriasari *et al.,* 2010).

These researchs demonstrate the potential of NAR as chemopreventive agent. However due to its poor solubility, its absorption capability into the body is also poor. An interesting technique to overcome this condition is nanoencapsulation, therefore the bioavailability of NAR can be increased

through its pharmacokinetic as well as bio-distribution.

Nanoparticle using biodegradable polymer material such as chitosan (CS) has gained attention to be developed, particularly in the development of oncological therapy. CS is composed of 2 sub-units of D-Glukosamin and N-asetil-D-glukosamin which are bound together by (1,4) glycosidic bond (LeHoux and Grondin, 1993; Rowe *et al.,* 2006). Amine group on glucosamine unit of CS is important part, because it gives high and reactive positive charge. Positive charge of CS is able to form complex along with anion compound. CS also can increase the transport of medicine that passes cell membrane (Winarti *et al.,* 2011; Martien and Loretz, 2007)

The formulation of CS with NAR on this research becomes nanoparticle that is expected to provide high intracellular uptake due to its unique sub-cellular size compared to the microscopic system (Mosquera *et al*., 2001). Therefore, the potential of being anti-cancer can be increased compared to the use of the initial compound, which in this case is NAR.

MATERIAL AND METHODS

Low viscous CS [2-amino-2-deoxy-(1→4)-β-D glucopyranan] p.a, Pentasodium tripolyphosphate (TPP) p.a, and NAR ≥95% p.a which were obtained from Sigma, Germany. MTT [3-(4,5-dimethylthiazol-2-yl)-2,5-diphenyl tetrazolium bromide], DMEM, and FBS which were ordered from Sigma-Aldrich, T47D cell line which is obtained from Parasitology Laboratories, Faculty of Medicine, University of Gadjah Mada, Yogyakarta. Other chemicals were in analytical grade.

Preparation of CS nanoparticles

CS nanoparticles was prepared through ionic gelation method (Calvo *et al.,* 1997) with some modification. CS solutions (0.02%; 0.04%; 0.06%; 0.08%; 0.10% w/v) were prepared by dissolving CS in acetic acid (0.15%v/v). TPP solution (0.1%w/v) is prepared by dissolving in double distilled water. CS nanoparticles were prepared by adding 6mL of TPP solutions and 3.6mL of Tween-80 (0.01%v/v) as an emulsifier dropwise into 30mL of CS solution under a constant magnetic stirring at 1000rpm. The nanoparticles were formed by ionic interaction of CS and TPP as cross-linker.

Preparation of NARNPs

To mix drug with CS nanoparticles, the pure NAR powder was dissolved into 96% of ethanol to produce 0.2%w/v NAR solution. Afterward, the NAR solution was then mixed with 0.02%; 0.04%; 0.06%; 0.08%; and 0.10% w/v CS solutions under magnetic stirring. Then, 1.5mL of TPP solution (0.1%w/v) and 1.075mL of Tween-80 solution (0.01%v/v) were added dropwise into mixtures under magnetic stirring at 1000rpm, and NAR loaded CS nanoparticles were simultaneously obtained.

Physical characterization of nanoparticles

Evaluation of encapsulation efficiency (EE)

EE of NAR was determined by measuring the ultraviolet (UV) absorption of the each supernatan of NARNPs which is obtained after ultracentrifugation. The corresponding calibration curves were made by subjecting the supernatants of standards NAR solutions (5; 10; 15; 20; 25ppm) under UV/Vis spectro-photometer (Shimadzu, Japan). NAR is measured at 290nm (λ_{max}). EE of NAR is calculated according to the following formula:

$$\text{Entrapment efficiency (EE) (\%)} = \frac{Wt - Wf}{Wt} x\ 100 \quad .....(1)$$

Meanwhile, Wt is the total initial amount of NAR and Wf is the amount of free NAR in the supernatant after ultracentrifugation (15.000rpm, 80min). All measurement were performed in triplicate and results were reported as mean ± standard deviation.

Particle Size and Particle Size Distribution

The result of cross-linked CS nanoparticles were then analyzed for mean particles size and particle size distribution by *Delsa™ Nano Submicron Particle size*. Five mL of aquadest is added to 2 drops of NARNPs and 3mL of the mixture is taken and put into cuvette to be analysed.

Determination of zeta (ζ) Potential

Zeta potential measurement of NARNPs dispersion were performed by using a *Delsa™ Nano Submicron Particle size* at 25°C. The zeta

potential value was measured at the default parameters of dielectric constant, refractive index, and viscosity of water. The sampling time was set to automatic.

Morphology of nanoparticles

Drops of 10mL of freshly prepared nanoparticle solution were placed on pioloform coated grids and dried for 15 min. The fluid was removed while the dried nanoparticles remaining on the grids. These grids were dried and examined by transmission electron microscope (JOEL-JEM 1400, Japan) with an in-column energy filter (EFTEM). Therefore, it was analyzed 120kV of nanoparticles energy loss, which depends on their density. Digital micrographs were obtained from TEM digital imaging/ scanning circuitry which displays TEM images.

FTIR analysis

The FTIR spectrum of the specimen is recorded with infrared spectrophotometer. FTIR spectra were taken in the wavelength region of 4000 to 400 cm^{-1} at room temperature by using potassium bromide pellets (Merck, IR grade) for CS, TPP, NAR, and NARNPs. The samples were allowed to form pellets at pressure of 10.3 x 10^4 Pa.

Differential Scanning Calorimetry (DSC)

The termal behavior of the NAR and NARNPs were characterized by DSC (Mettler Toledo DSC). Approximately 3 to 6mg of the freezed dried particles were weighed into an aluminium pan. The nanoparticles were heated from 30 to 360°C at a heating rate of 10°C/min per cycle. To maintain inert atmosphere, nitrogen was purged at the flow rate of 20cc/min.

Observation of the Cellular Uptake

T47D cells were seeded in six-well plates with cover slip which was coated at the bottom of the well. The cells were incubated in CO_2 incubator until starvation. Cells media was replaced with a new media. 1000uL of NAR nanoparticle was added afterwards, then incubated. After incubation as long as 24h, methanol was added for 30s then discarded right away. Cover slip containing the cells were attached on the object glass and then observed through a fluorescent microscope (Zeiss).

In vitro cytotoxicity assay

Cytotoxicity of NARNPs was studied against T47D cells. T47D cells were cultured in Dulbecco's modified Eagle's medium (DMEM) (Sigma) supplemented with 10% FBS. The cells culture medium was maintained at 37°C in a humidified incubator which contains 5% of CO_2. Trypsinized confluent cells monolayer (75-80%) and the cells in the exponentially growing phase were used for cytotoxicity experiments.

MTT assay for *in vitro* cell viability studies

The cytotoxicity assay of NARNPs against T47D cells was evaluated by using MTT assay. The cytotoxicity of the nanoparticles was determined after 24h incubation with T47D cells. The cells were plated at a density of 5×10^3 cells/well (optimal seeding density) in 96 well plates at 37°C in 5% CO_2. The purpose was to determine cells viability.

After 12h of incubation was performed, the medium in the wells was replaced with the fresh medium containing nanoparticles of 1000µM NARconcentrations. After 24h, MTT dye solution (20µL, 5mg/mL in phosphate buffer pH-7.4) was added to each well. The incubation was further continued for another 2h at 37°C and 5% of CO_2 for exponentially growing cells. The medium in each well containing unbound MTT and dead cells was removed by suctioning process. The formazan crystals were solubilized with 100µL of DMSO, and the solution was optimally mixed to dissolve the reacted dye. The absorbance of each well was readable to a microplate reader at 540nm. The control experimental medium did not contain nanoparticles. Blank CS nanoparticles were used in evaluating its effect to cells viability. The spectro-photometer was calibrated to zero absorbance by using culture medium with no cells. The relative cell viability (%) associated to control wells containing cell culture medium without nanoparticles was calculated by :

[A]test/[A] control × 100.....(2)

where [A]test was the absorbance of the test sample and [A]control was the absorbance of control sample.

Apoptosis assay

T47D cells of $5x10^4$/mL were distributed into 24-well plate previously coated with cover slip at the bottom followed by incubation until returning to normal. Cells were treated with NARNPs and incubated for 15h. These cells were washed slowly at the end of the incubation and cover slip containing the cells was then transferred to the top of the slide and it was added 10mL of reagent AE. The cells were then observed under a fluorescent microscope as soon as possible after the reagent becomes dry.

RESULTS AND DISCUSSION

Nanoparticles formulation selection

Formulation optimization of NARNPs was conducted by mixing CS solution with a concentration of 0.02, 0.04, 0.06, 0.08, and 0.1% to NAR solution with a concentration of 0.2% in this preliminary experiment. These five formula was stored for 3 days long at room temperature (Winarti *et al.,* 2011; Martien and Loretz, 2007). The purpose was to observe the formation of sediment. Nanoparticles with CS concentration of 0.06, 0.08, 0.10% were the most stable until 3 days, therefore these three formula were chosen for further characterization.

Encapsulation Efficiency (EE) of NARNPs

EE evaluation was conducted by spectrophotometer UV-Vis measured at 290nm (λ_{max}). The EE of NARNPs increased by the way of increasing the concentration of CS as shown in Table I. The EE for NARNPs were on the range of 42.22±0.696-64.45±0.028%. Meanwhile, increasing CS concentration from 0.08% to 0.10% do not increase EE because the effect of CS-TPP mass ratio. The obtained results were in accordance with previous researches of catechins delivery. It was mentioned that the encapsulation efficiency of tea catechins decreases from 45.14 to 32.23% as the CS-TPP mass ratio increases from 4:1 to 9:1 (Hu *et al.,* 2012).

Characterization of NARNPs using Particle Size Analyzer and Zeta Sizer

Dynamic light scattering measure the zeta potential and particle size distribution. The particle size of NARNPs increases through increasing the CS concentration from 0.06% to 0.1%w/v. The increase in particle size was possibly because of the presence of intermolecular hydrogen bonding (due to −OH groups) and intermolecular electrostatic repulsion (due to −NH3+ groups) existing at the contour of CS (Qun and Ajun, 2006). When the concentration of CS increases, more molecules of CS tend to entrap NAR and crosslink with counter ion (TPP) to form a single larger particle (Fan *et al.,* 2012). This fact was revealed in the data obtained in the research and presented on table II.

ζ-potential was an index used to measure the stability of the nanoparticles. In most cases the higher the value of ζ-potential the larger the amount of charge on their surface, which leads to strong repulsive interaction among the nanoparticles, as the result the stability of the nanoparticles becomes higher (Lee, 2007). In the current study, positive ζ-potential was indicated by NARNPs use of 0.06%; 0.08%; and 0.10% CS and the zeta value ranges from +29.78 to +35.72mV. The ζ-potential of the NARNPs was summarized in table II. The data also demonstrates that the zeta potential of CS nanoparticles was significantly increased by increasing the CS concentration.

Morphology of NARNPs

Morphology of different NARNPs was investigated by using TEM. The morphology of NARNPs was found to be influenced by the concentration of chitosan. Chitosan with a concentration of 0.10% produce the biggest mean particles compared to chitosan with concentration of 0.06% and 0.08% as depicted by Figures 1(a) to 1(f) respectively. Results (Figure 1) generally showed that the shape of the nanoparticles was fairly spherical. The spherical shape make NARNPs more easy to be taken up by the cells than rod shape.

When compared with the results of measurements using the particle size analyzer (PSA), a visible difference in size was obtained

Table I. % EE of NARNPs at various concentrations of CS (Mean ±S.D, *n* = 3)

No	CS concentration (%)	EE (%)
1.	0.06	42.22±0.696
2.	0.08	64.45±0.028
3.	0.10	59.07±0.543

Table II. Dynamic Light Scattering and Zeta Potential Analysis of NARNPs

No.	Cs concentration (%)	Size (nm) X ± SD	Zeta Potential (mV)
1.	0.06%	469.6±135.2	29.78±0.89
2.	0.08%	750.8±207.4	35.72±0.64
3.	0.10%	564.0±158.2	32.77±0.64

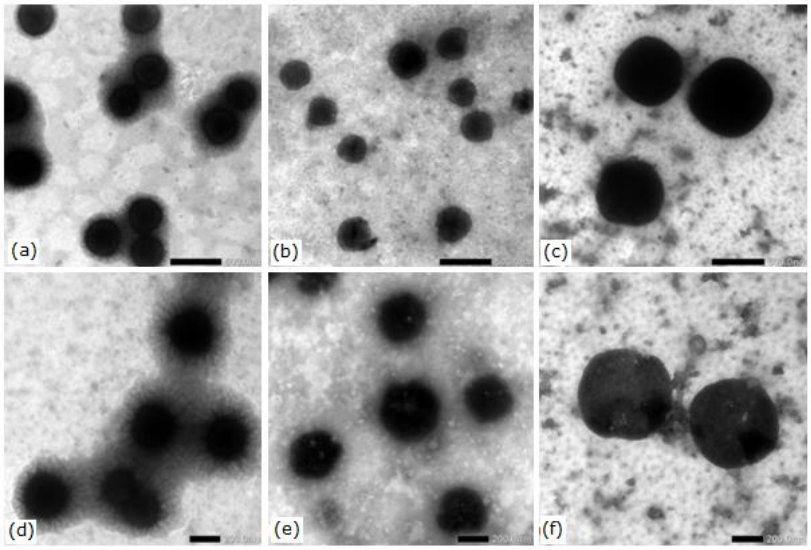

Figure 1. TEM images of NARNPs (a) chitosan of 0.06%-10.000x magnification; (b) chitosan of 0.08%-10.000x magnification; (c) chitosan of 0.10%-10.000x magnification; (d) chitosan of 0.06%-15.000x magnification; (e) chitosan of 0.08%-15.000x magnification; (f) chitosan of 0.10%-15.000x magnification.

by using TEM. This was caused by the diameter obtained from measurements using PSA shows the hydrodynamic diameter of the liquid medium, while the TEM measurements shows the diameter of the nanoparticles in dry conditions (Peng *et al.,* 2005)

FT-IR Analysis

NARNPs were prepared between chitosan and tripolyphosphate (TPP) by ionic gelation method. FTIR spectra of NARNPs were taken with potassium bromide pellets. FTIR studies of CS, NAR, Sodium TPP and NARNPs were performed to characterize the chemical structure of nanoparticles. FTIR spectra of CS, NAR, Sodium TPP and NARNPs were shown in figure 2. The strong and wide peak in the 3500-3300 area was attributed to hydrogen-bonded O-H stretching vibration in the CS spectra. The peaks of N-H that stretchs from primary amine and type II amide were overlapped in the same region. The peak for asymmetric stretch of C-O-C was found approximately at 1249cm^{-1}. In CS-TPP nanoparticles the tip of the peak of 3400cm^{-1} has a shift to 3435cm^{-1} and gets wider with increased relative intensity indicating an enhancement of hydrogen bonding.

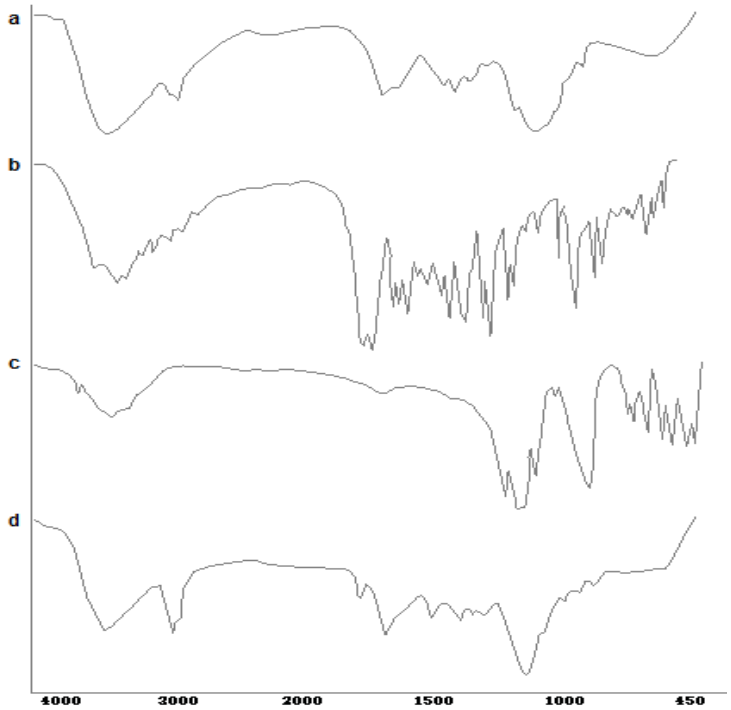

Figure 2. FT-IR of (a) CS, (b) NAR, (c) TPP, (d) NARNPS

In nanoparticles the peaks for N-H bending vibration of amine I at 1650cm^{-1} shifted and split to 1640cm^{-1} and 1603cm^{-1}. The crosslinked CS also indicates a P=O peak at 1157cm^{-1}. The results were associated to the linkage between phosphoric and ammonium ion, it was indicated that the tripolyphosphoric groups of TPP were linked with ammonium groups of CS.

Differential Scanning Calorimetry (DSC) Analysis

Thermal analysis indicated that the DSC scan of the drug presented a sharp endothermic peak corresponding to its melting transition temperature. The DSC spectrum of the NAR showed a sharp endothermic peak with heating enthalpy 261.1716 J/g. Figure 3a, 3b, 3c and 3d illustrates DSC thermogram of NAR, CS, TPP, and NARNPs respectively. DSC spectrum of NARNPs does not exhibit the distinct peak of NAR from that conclusion it was described that in the NARNPs drug was in partial crystalline condition and there was no interaction between drug and polymer.

Cellular Uptakes Determination

In purpose to see the ability of the nanoparticles in entering the cells, then Cellular uptake was examined. The complex coaservation method used to bind the positive charge of CS and the negative charge of Na-TPP allow the nanoparticles to bind with the negative charged plasma membrane, continued with endocytosis process, and at last the nanoparticles enter the cells.

Cellular uptake was examined using Fluorescent microscopy (Figure 4). Colors ranging from green to yellow will be produced by NAR because of the chromophore group in this molecule. This result proves that the formulated NAR penetrates well into the cells. When being observed, the cells become fluorescent. The observation using fluorescent microscopy demonstrates that the NAR nanoparticles at CS concentration of 0.06%, 0.08%, and 0.1% provide a higher intensity of the green to yellow fluorescent when it was compared to the free NAR.

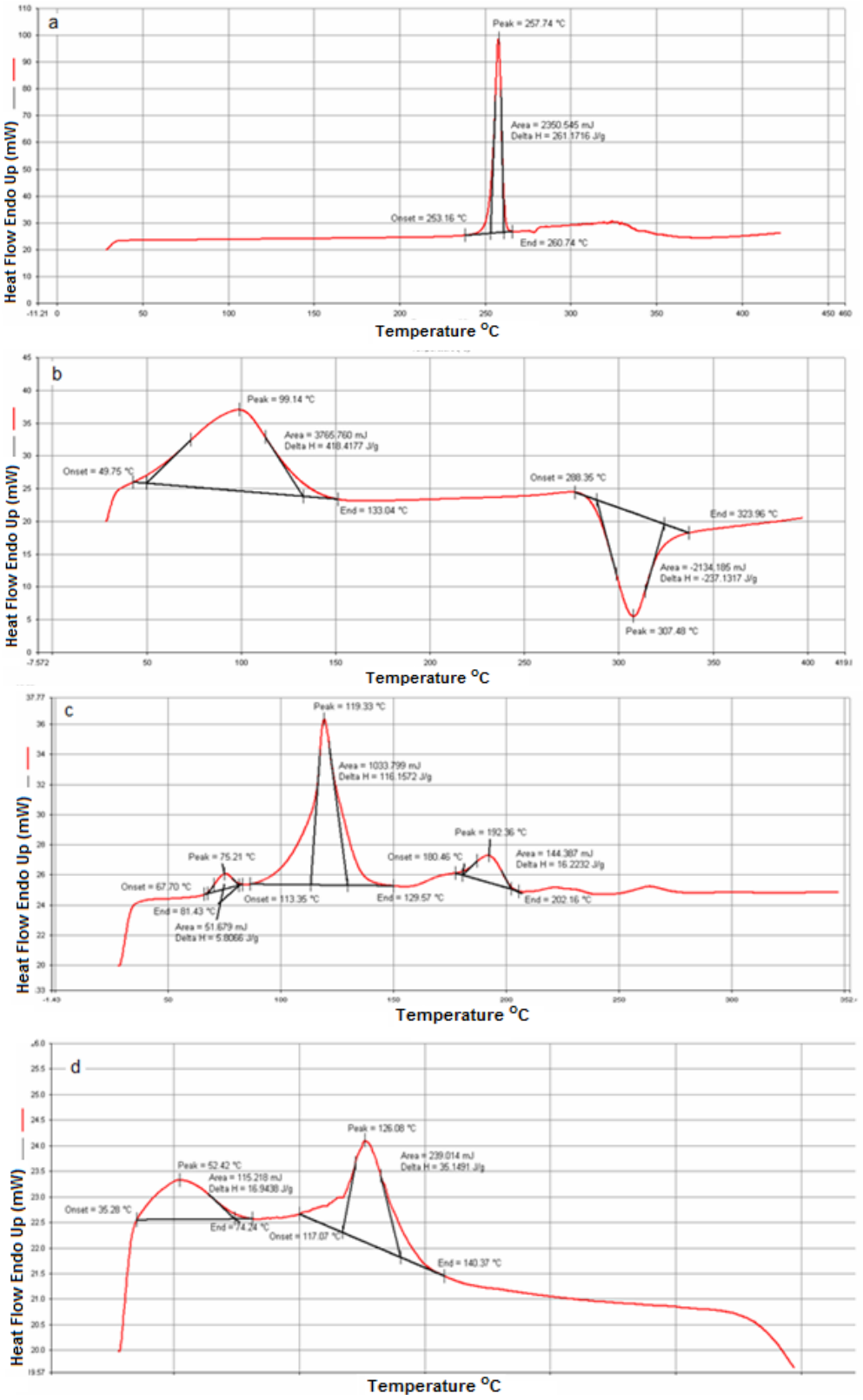

Figure 3. DSC thermogram of (a) NAR, (b) CS, (c) TPP, and (d) NARNPs.

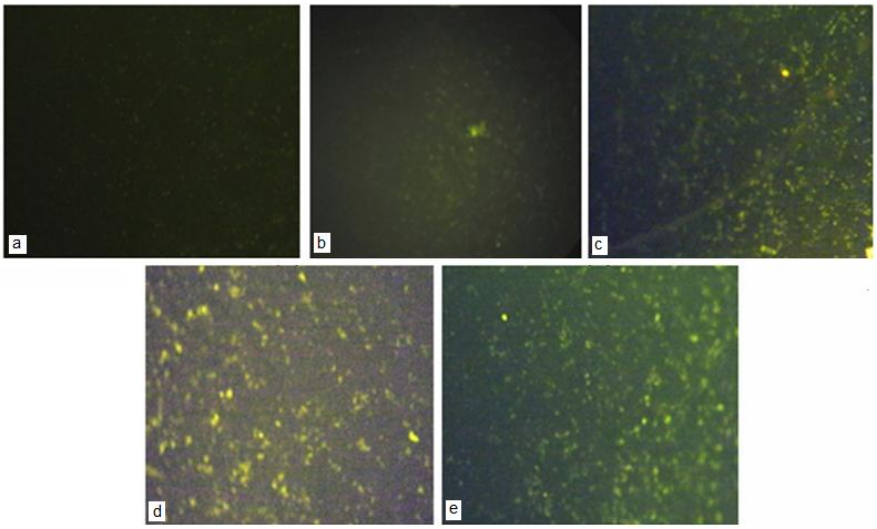

Figure 4. Cellular uptake studies of NARNPs using fluorescence microscope. (A) control cell; (B) Free Naringenin; (C) NARNPs with chitosan of 0.06%; (D) NARNPs with chitosan of 0.08%; (E) NARNPs with chitosan of 0.10%-100x magnification. Qualitatively assayed by visual asessment. NAR will give a green to yellow fluorescent due to the chromophore group in this molecule.

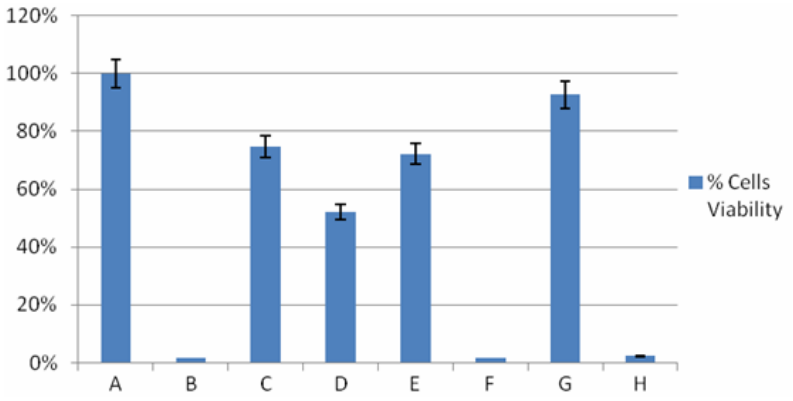

Figure 5. Viability of T47D cells in cell culture with (A) Control cell; (B) Free Naringenin; (C) Blank Nanoparticles of chitosan 0.06%; (D) NARNPs with chitosan of 0.06%; (E) Blank Nanoparticles of Chitosan 0.08%; (F) NARNPs with chitosan of 0.08%; (G) Blank Nanoparticles of Chitosan 0.10%; (H) NARNPs with chitosan of 0.10% and incubation time (overnight) OVN. Viability of untreated cells was considered 100%. Each point represents the mean±SD of three determinations.

MTT Assay

To determine the level of NARNPs cytotoxicity against T47D cell line as the model of breast cancer cells, cytotoxic test was conducted. This test method was based on the conversion of yellow tetrazolium salt by succinate hydrogenase in mitochondria into formazan crystals (Mossmann, 1983). The purple color obtained from formazan form was proportional to the number of living cells that was able to be measured through ELISA reader.

NAR which has anticancer activities with IC_{50} value of 509μM gives the toxic effect on the cancer cells line. The results (Figure 5) demonstrate that NARNPs with CS of 0.08%

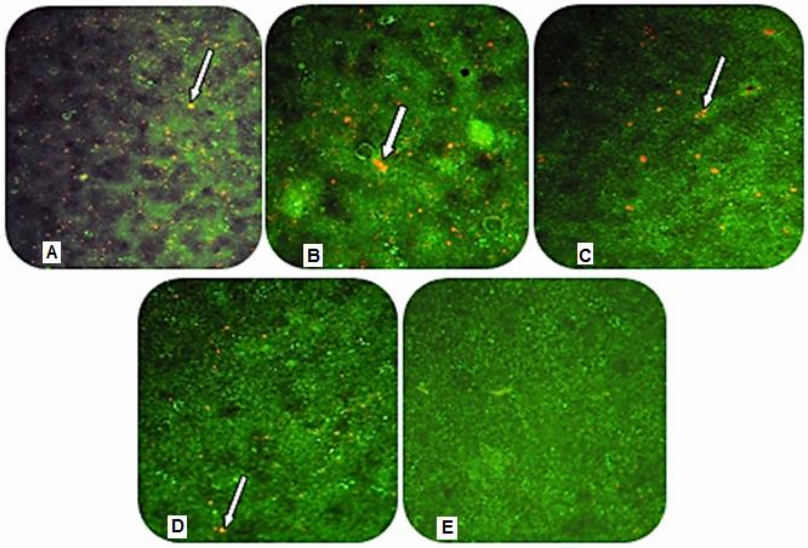

Figure 6. Apoptosis assay against T47D cells line; (A) Free naringenin; (B) NARNPs with chitosan of 0.06%; (C) NARNPs with chitosan of 0.08%; (D) NARNPs with chitosan of 0.10%; (E) Control cell. DNA was stainned using acridine orange-etidium bromide and the pictures were taken under fluorescent microscope-100x magnification. Apoptosis cells (pointed by the arrow) gave an orange fluorescent.

has higher toxicity effect on T47D cell line compared to the free NAR after 24h incubation. Nanoparticle formulation increases the uptake of NAR into the cell as well as increases the effect of anti-cancer.

NARNPs with CS of 0.08% also have the highest EE and zeta potential among other NARNPs formula, hence its cytotoxicity effect was better than NARNPs with CS of 0.06% and 0.10%. Higher zeta potential make NARNPs easier to enter the cells, therefore more NAR can be delivered inside the cells to induce cytotoxicity.

Apoptosis Assay

Treatment of free NAR and NARNPs with CS concentration of 0.06%; 0.08%; and 0.10% were capable of stimulating apoptosis in T47D cells with an almost similar orange fluorescence intensity (Figure 6). The ability of inducing apoptosis was analyzed qualitatively by evaluating orange color in the cells. Based on the observation of its morphology, both free NAR and NARNPs show nucleus cells fragmentation. Increasing signs of apoptosis was higher in free NAR when it compared to cells treated by NARNPs. It was because of crosslink between the CS and Na-TPP which causes increasing viscosity of polymer, so that the release mechanism through diffusion to the polymer was slower. This system was considered appropriate to control drug release. Observations need to be performed not only in overnight incubation. Nanoparticles with sustained release system was more suitableas a carrier of therapeutic agents for the treatment of cancer because of the risk of resistancy and adverse side effects on healthy cells. In addition, the presence of surface charge causes accumulation into cells through endocytosis and more specific distribution of cytotoxic active ingredients, thus reducing side effects. The size of a nanoparticle drug delivery system also causes the distribution towards smaller cells more easily and can be avoided by the reticulo endothelial clearance.

CONCLUSION

Chitosan nanoparticles–TPP conjugates have the capability to encapsulate naringenin hence increase the cellular uptake and cytotoxcicity of naringenin against T47D cells line. NARNPs also can induce the apoptosis effect.

ACKNOWLEDGEMENT

Researchers gratefully thank to DIKTI (Directorate of Higher Education) Ministry of Education, Indonesia through "Hibah Bersaing" for financial support in this research.

REFERENCES

Anbarassan B., Vennya VM., Niranjana VA., and Ramaprabhu S., 2013. Optimization of The Formulation and In-vitro Evaluation of Chloroquine Loaded Chitosan Nanoparticles Using Ionic Gelation Method. *J.Chem.Pharm.Sci.*6(1): 66-72

Calvo P., Remuñán-López C., Vila-Jato JL., and Alonso MJ., 1997. Novel hydrophilic chitosan-polyethylene oxide nano-particles as protein carriers. *Journal of Applied Polymer Science*.63(1):125–132.

Chang H., Mi M., Ling W., Zhu J., Zhang Q., Wei N., Zhou Y., Tang Y., and Yuan J., 2008. Structurally Related Cytotoxic Effects of Flavonoids on Human Cancer Cells in Vitro. *Arch. Pharm. Res.* 31(9):1137-1144.

De Leo F., De Bosco SF., 2005. Citrus Flavonoids as Bioactive Compounds: Role, Bioavailability, Socio-economic Impact and Biotechnological Approach For Their Modification. *9th ICABR International Conference on Agricultural Biotechnology: Ten Years Later*. Rovello. Italy

Dembinski A., Warzecha Z., Konturek SJ., Ceranowicz P., Dembinski M., Pawlik WW., Kusnierz-Cabala B., and Naskalski JW., 2004. Extract of grapefruit-seed reduces acute pancreatitis induced by ischemia/reperfusion in rats: possible implication of tissue antioxidants. *J. Physiol. Pharmacol.* 55:811

Erlund I., Meririnne E., Alfthan G., and Aro A., 2001. Plasma kinetics and urinary excretion of the flavanones naringenin and hesperetin in humans after ingestion of orange juice and grapefruit juice. *J. Nutr.* 131:235

Fan W., Yan W., Xu Z., and Ni H., 2012. Formation mechanism of monodisperse, low molecular weight chitosan nanoparticles by ionic gelation technique. *Colloids and Surfaces B.* 90:21–27.

Fitriasari A., Susidarti RA., and Meiyanto E., 2010. Peningkatan Efek Sitotoksik Doxorubicin oleh Naringenin Melalui Pemacuan Apoptosis Sel kanker Payudara MCF-7. *Jurnal Bahan Alam Indonesia*. 7 : 3

Gopalakrishnan A., Xu CJ., Nair SS., Chen C., Hebbar V., and Kong AN., 2006. Modulation of activator protein-1 (AP-1) and MAPK pathway by flavonoids in human prostate cancer PC3 cells.*Arch. Pharmacol. Res.* 29: 633-644

Hu B., Ting Y., Yang X., Tang W., Zeng X., and Huang Q., 2012. Nanochemo-prevention by Encapsulation of (-)-epigallocathecin-3-gallate with Bioactive Peptides/Chitosan Nanoparticles for Enhancement of its Bioavailability. *Int. J. Mol. Sci.*13: 14251-14261

Junedi S., Susidarti RA., and Meiyanto E., 2010. Peningkatan Efek Sitotoksik Doxorubicin oleh Naringenin pada Sel Kanker Payudara T47D Melalui Induksi Apoptosis. *Tesis*. Fakultas Farmasi Universitas Gadjah Mada.

Kanno S., Tomizawa A., Hiura A., Osanai A., Shouji A., Ujibe A., Ohtake AT., Kimura K., and Ishikawa M., 2005. Inhibitory Effect of Naringenin on Tumor Growth in Human Cancer Cell Line and Sarcoma S-180-Implanted Mice. *Biol. Pharm. Bull.* 28(3): 527-530

Kanno S., Tomizawa A., Ohtake T., Koiwai K., Ujibe M., and Ishikawa M., 2006. Naringenin induce apoptosis via activation of NF-κB and necrosis involving in the loss of ATP in Human Promyeloleukimia HL-60 cells.*Toxicol.Lett*. 166: 131-139

Le Gall G., DuPont MS., Mellon FA., Davis AL., Collins GJ., Verhoeyen ME., and Colquhoun IJ., 2003. Characterization and content of flavonoid glycosides in genetically modified tomato (Lycopersicon esculentum) fruits. *J. Agric. Food. Chem.*51:2438

Lee YK., 2007.Chitosan and Its Derivatives for Gene Delivery, *Macromolecular Res.*15(3):195-201

LeHoux JG., and Grondin F., 1993. Some Effects of Chitosan on Liver Function in The Rat. *Endocrinology*.132: 1078-1084

Martien R., Loretz B., 2007.Chitosan Thioglycolic Acid Conjugate: An Alternative Carrier for Oral Nonviral Gene Delivery? *J. Biomed. Mater Res. A*.82(1):1-9

Mokarram RA., Alonso MJ., 2006. Preparation and Evaluation of Chitosan Nanoparticles Containing Diphteria Toxoid as New Carriers for Nasal Vaccine Delivery In Mice. *Archieves of Razi Institute*.61(1): 13-25

Mosqueira V., Legrand P., Gulik A., Bourdon O., Gref R., Labarre D., and Barratt G., 2001. Relationship Between Complement Activation, Cellular Uptake and Surface Physicochemical Aspects of Novel PEG-modified Nanocapsules. *Biomaterials*. 22:2967-79

Mossmann T., 1983. Rapid Colorimetric Assay for Cellular Growth and Survival: Application to Proliferation and Cytotoxicity Assays. *J. Immunol. Meth*. 65:55–63.

Peng J., Xing X., Wang K., Tan W., He X., and Huang S., 2005. Influence of Anions on The Formation and Properties of Chitosan-DNA Nanoparticles. J. *Nanosci. Nanotechnol*.5:713-7

Qun G., Ajun W., 2006. Effects of molecular weight, degree of acetylation and ionic strength on surface tension of chitosan in dilute solution. *Carbohydrate Polymers*.64(1): 29–36.

Rowe RC., Sheskey PJ., Owen SC., 2006. Chitosan. *HandBook of Pharmaceutical Excipients*, Pharmaceutical Press and American Pharmacist Association

Stark T., Bareuther S., and Hofmann T., 2005. Sensory-guided decomposition of roasted cocoa nibs (Theobroma cacao) and structure determination of taste-active polyphenols. *J. Agric.Food. Chem*. 53:5407

Thagele R., Mishra A., and Pathak AK., 2011. Formulation and Characterization of Clarithromycin Based Nanoparticulate Drug Delivery System.*Int.J.of Pharm.& Life Sci.(IJPLS)*. 2(1):510-115.

Tripoli E., Guardia ML., Giammanco S., Majo DD., and Giammanco M., 2007. Citrus flavonoids: Molecular structure, biological activity and nutritional properties: A review. *Food Chem*.104:466–479.

Wang H., Nair MG., Strasburg GM., Booren AM., and Gray JI., 1999. Antioxidant polyphenols from tart cherries (Prunus cerasus).*J. Agric. Food. Chem*. 47:840

Winarti L., Martien R., and Sismindari, 2011. Formulation of Nanoparticle from short chain chitosan as gene delivery system and transfection against T47D cell line. *Indonesian.J.Pharm*. 3(11):204-211

Xu Y., Hanna MA., 2007. Electrosprayed Bovine Serum Albumin-loaded Tripolyphosphate Cross-linked Chitosan Capsule, Synthesis and Characterization. *J.Microencapsul*. 24: 143-151

Zhang FY., Du GJ., Zhang L., Zhang CL., Lu WL., and Liang W., 2009. Naringenin Enhances the Anti-Tumor Effect of Doxorubicin Through Selectively Inhibiting the Activity of Multidrug Resistance-Associated Proteins but not P-glycoprotein. *Pharm. Res*. 26(4):914–924.